Supporting Information
Atomically Precise $Ag_{25}(SR)_{18}$ Nanoclusters: A Stable Photosensitizers for Photocatalysis

Linjian Zhan,[a] Junyi Zhang,[a] Boyuan Ning,[a] Yunhui He,[a,b]* Guangcan Xiao,[a,b] Zhixin Chen,[a,b] Fang-Xing Xiao[a,c]*

a. School of Advanced Manufacturing, Fuzhou University, Jinjiang, 362200, PR China.

b. Instrumental Measurement and Analysis Center, Fuzhou University, Fuzhou 350108, PR China

c. College of Materials Science and Engineering, Fuzhou University, Fuzhou 350108, PR China.

Email: hyh@fzu.edu.cn

fxxiao@fzu.edu.cn

Table of Content

Page NO.

Experimental Details

Materials

Cadmium acetate, ethylenediamine, CH_4N_2S, $CHCl_2$, $NaBH_4$, $AgNO_3$, distilled water, 2,4-dimethylbenzenethiol, PPh_4Br, methanol, 4-nitroaniline (4-NA), 3-nitroaniline (3-NA), 2-nitroaniline (2-NA), 4-nitrophenol (4-NP), 3-nitrophenol (3-NP), 2-nitrophenol (2-NP), 1-bromo-4-nitrobenzene, 1-chloro-4-nitrobenzene, 4-nitroanisole, 4-nitrotoluene (4-NT), nitrobenzene (NB), o-nitroacetophenone.

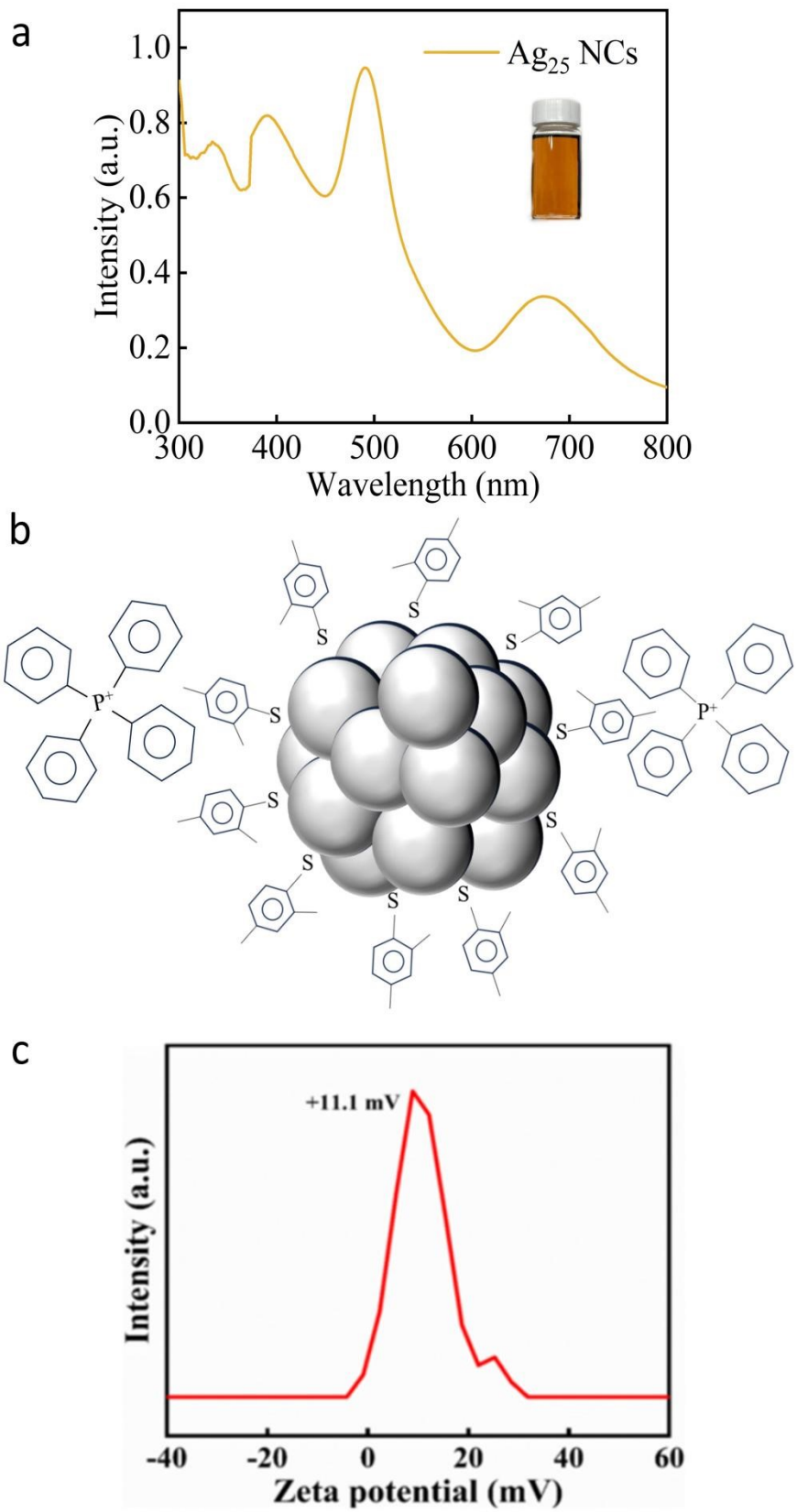

Fig. S1.(a) UV-vis absorption spectra of $Ag_{25}(SR)_{18}$ NCs and (b) schematic model illustrating the molecule structure of $Ag_{25}(SR)_{18}$ NCs and surface SR ligand, (c) Zeta potential of CdS NWs[1].

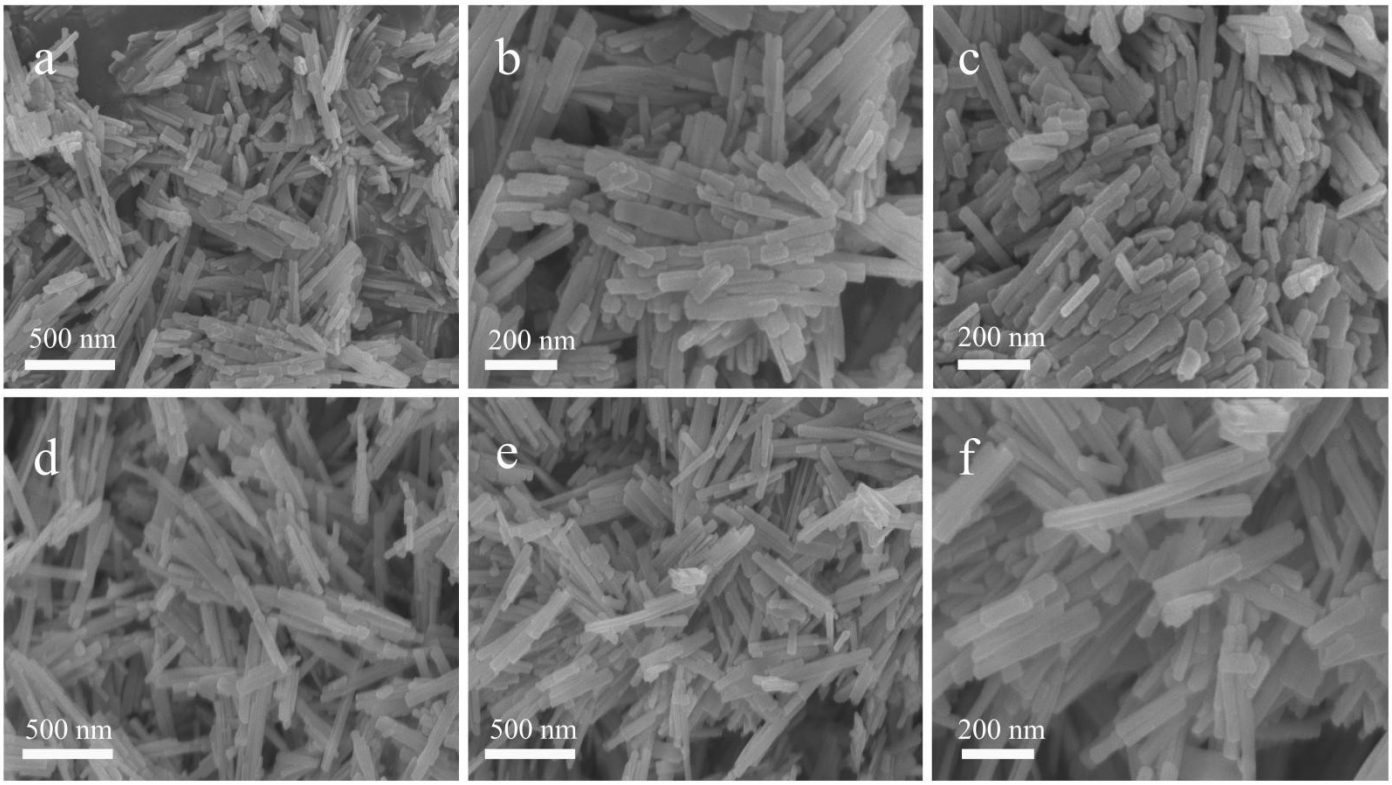

Fig. S2. FESEM images of (a-c) CdS NWs and (d-f) CdS/$Ag_{25}(SR)_{18}$ heterostructure.

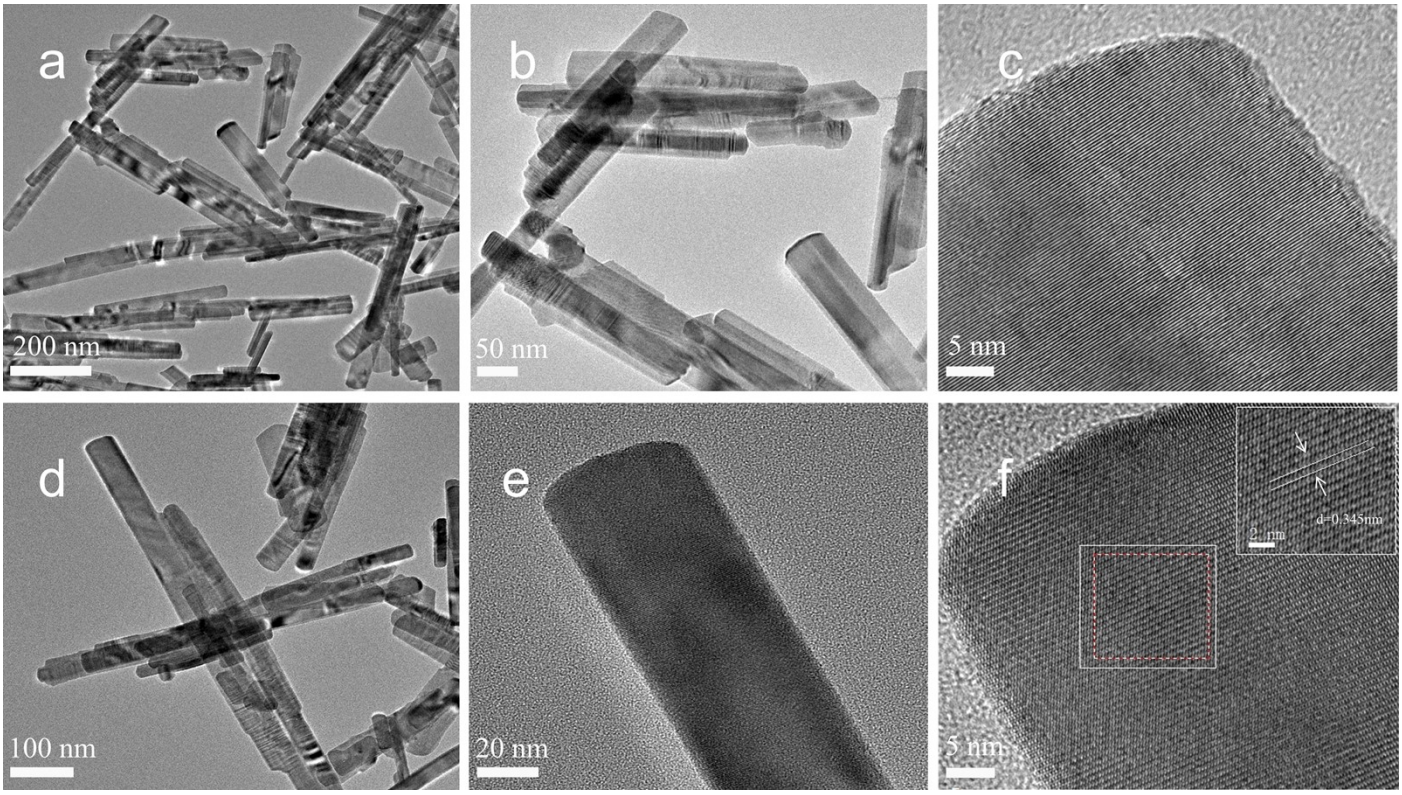

Fig. S3. TEM and HRTEM images of (a-c) CdS NWs and (d-f) CdS/$Ag_{25}(SR)_{18}$ heterostructure.

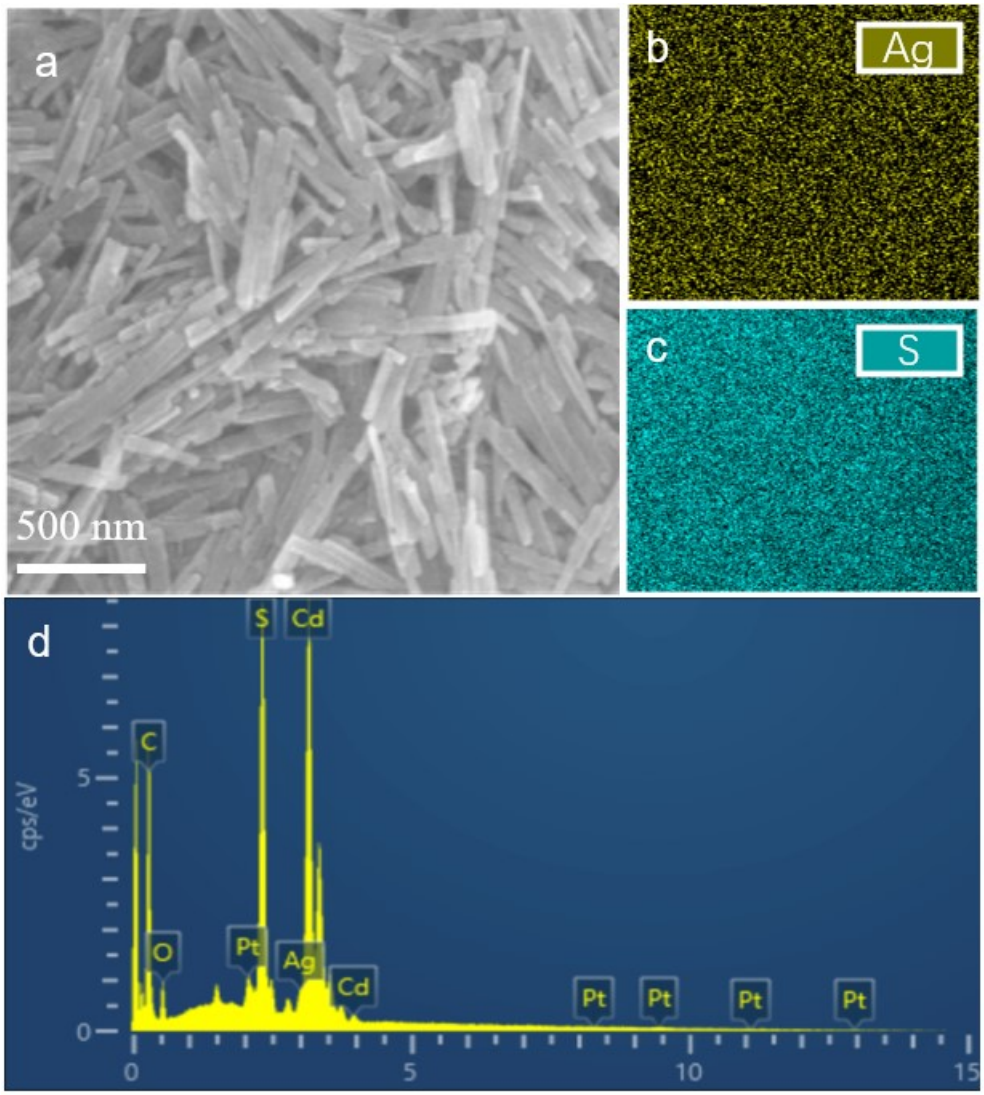

Fig. S4. (a) SEM image and (b-c) elemental mapping and (d) EDS results of CdS/$Ag_{25}(SR)_{18}$ heterostructure.

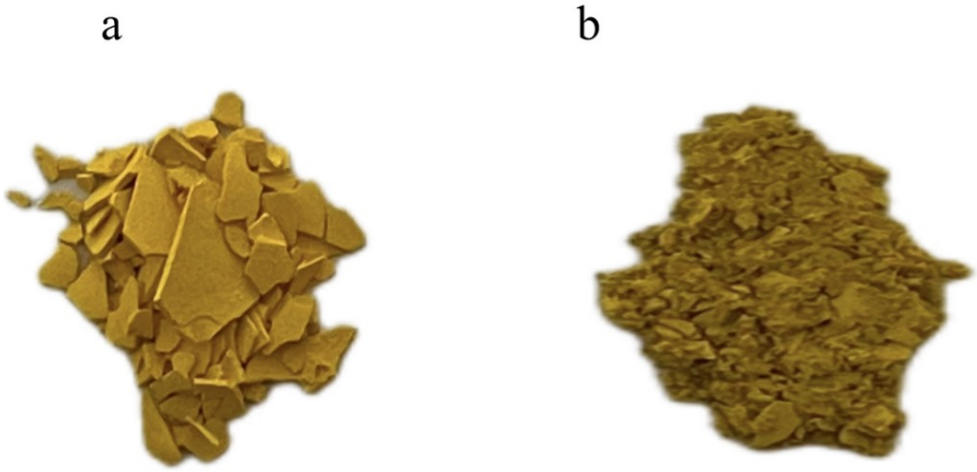

Fig. S5. Sample colors of (a) CdS NWs and (b) CdS/$Ag_{25}(SR)_{18}$ heterostructure.

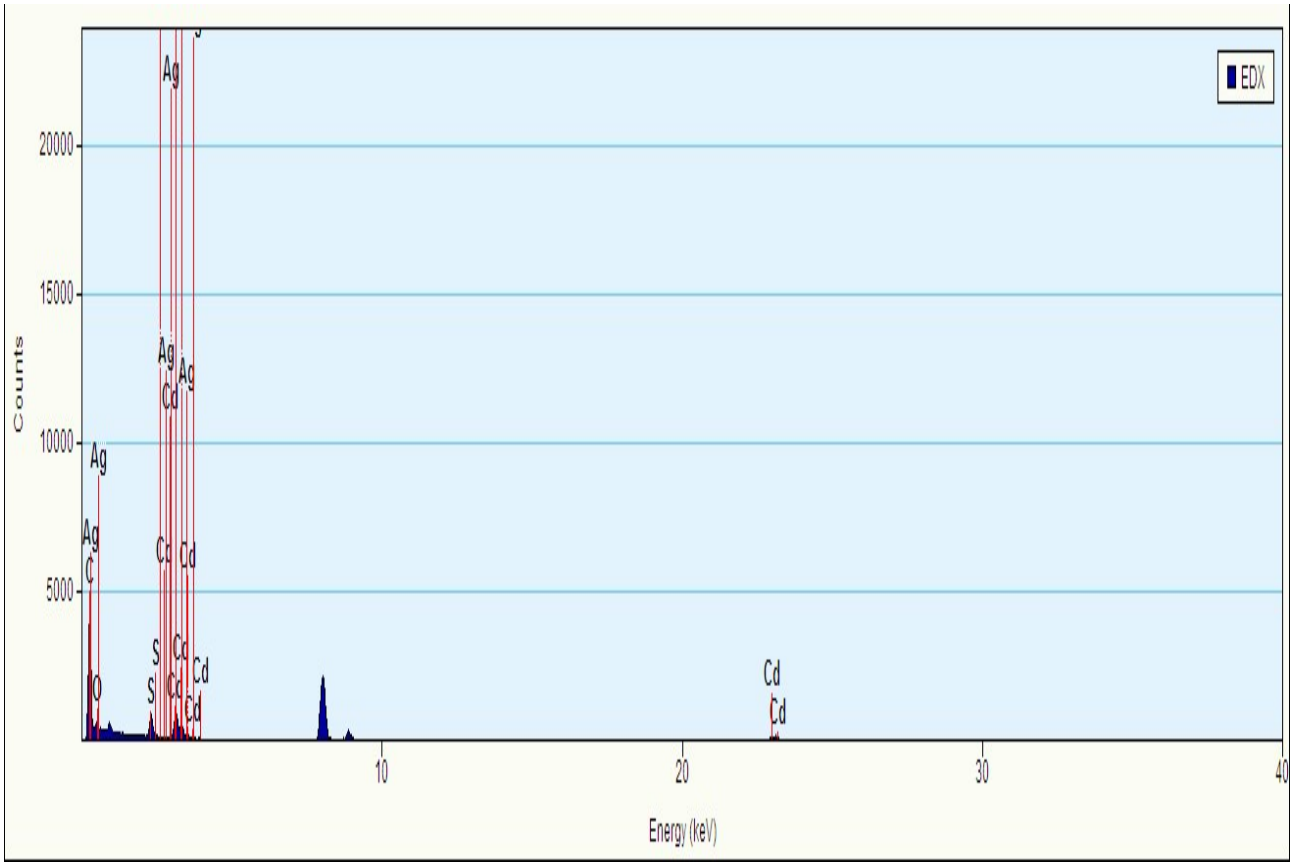

Fig. S6. EDS result of $CdS/Ag_{25}(SR)_{18}$ heterostructure.

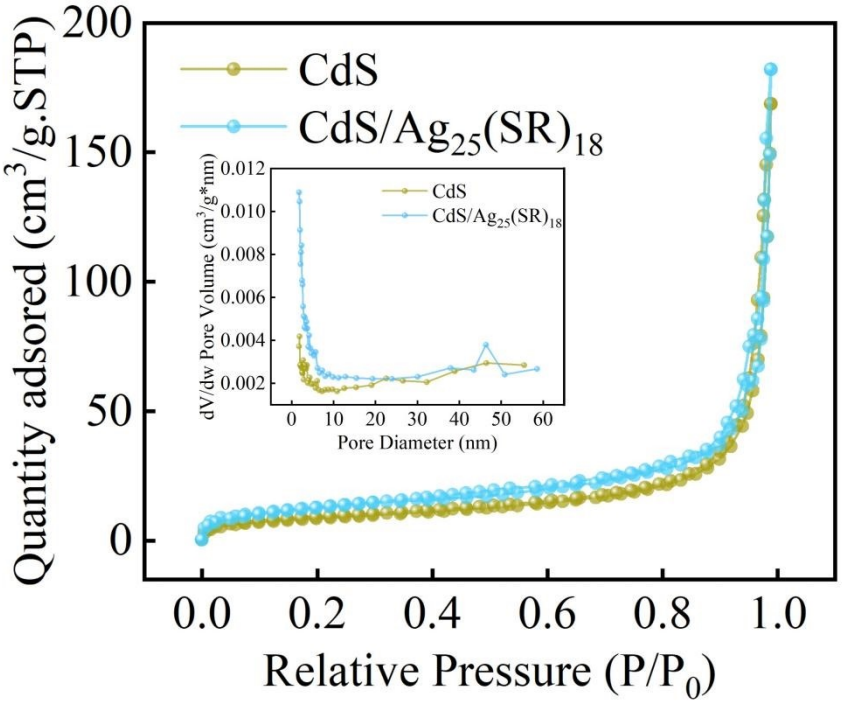

Fig. S7. Nitrogen adsorption-desorption isotherms of CdS NW and $CdS/Ag_{25}(SR)_{18}$ heterostructure with pore size distribution patterns in the inset.

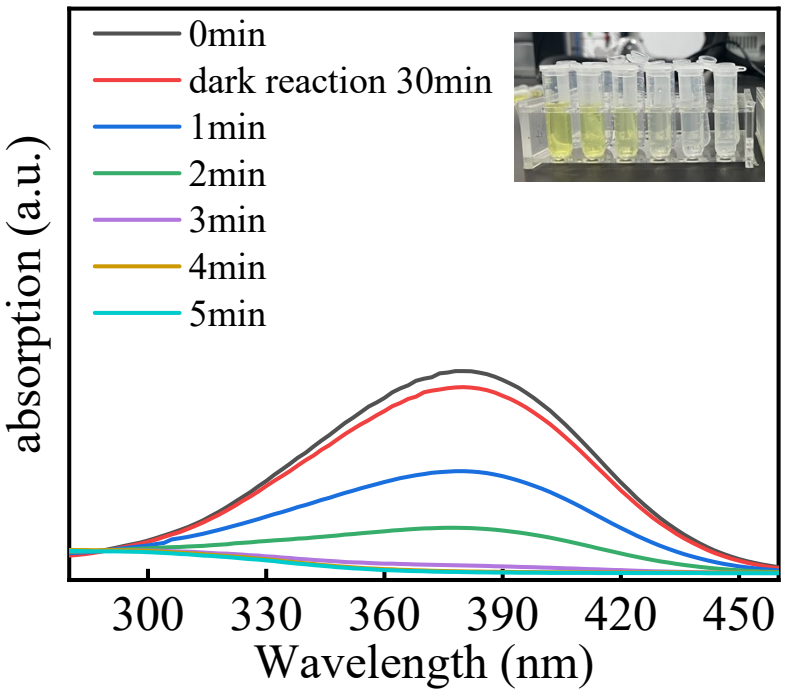

Fig. S8. UV-vis absorption spectra of 4-NA collected after designated irradiation time (1 min) when it was photoreduced over $CdS/Ag_{25}(SR)_{18}$ heterostructure under visible light irradiation ($\lambda > 420$ nm) with the addition of sodium sulfite as hole quencher and N_2 purge under ambient conditions.

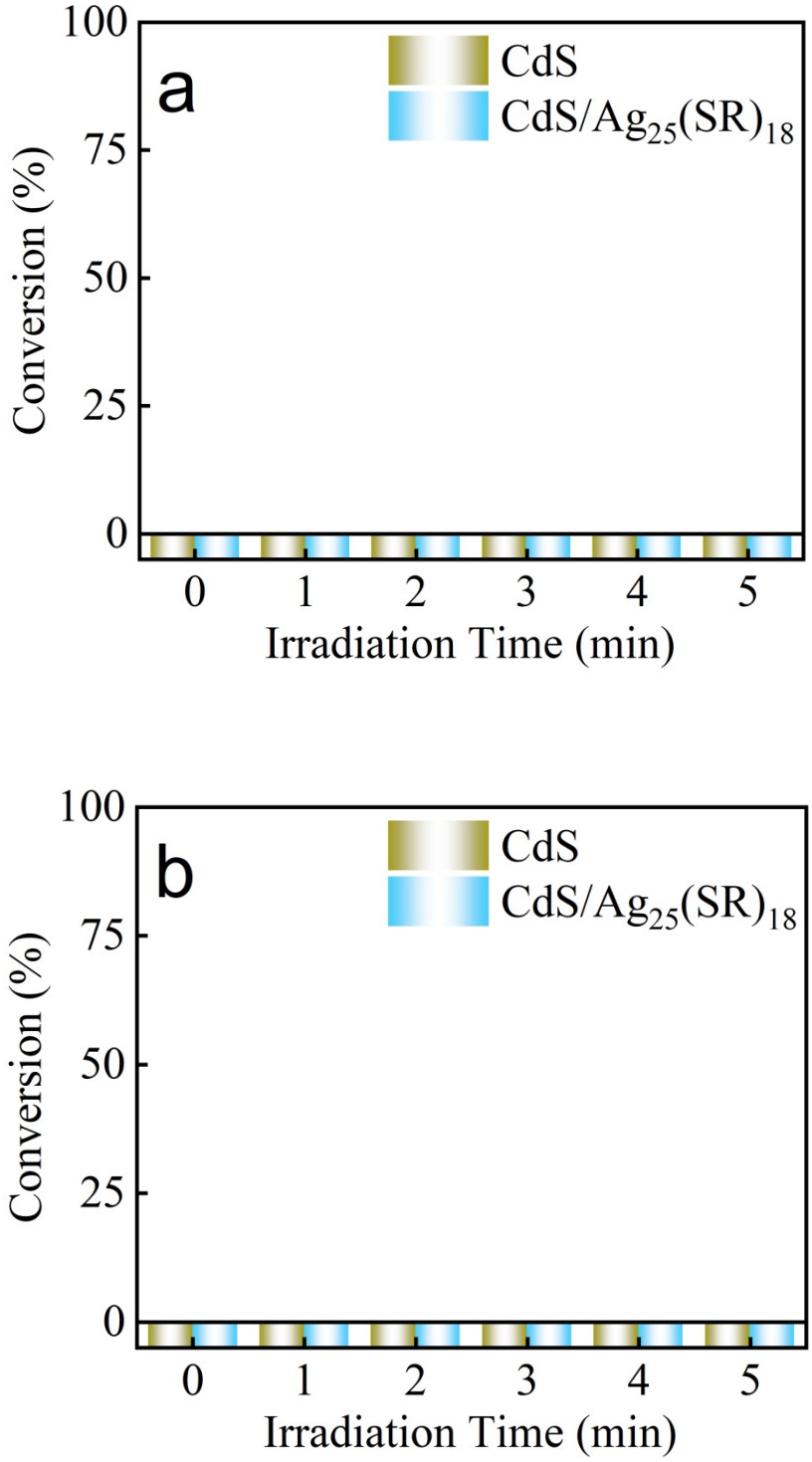

Fig. S9. Blank experiment for photocatalytic reduction of 4-NA (a) without light or (b) catalyst.

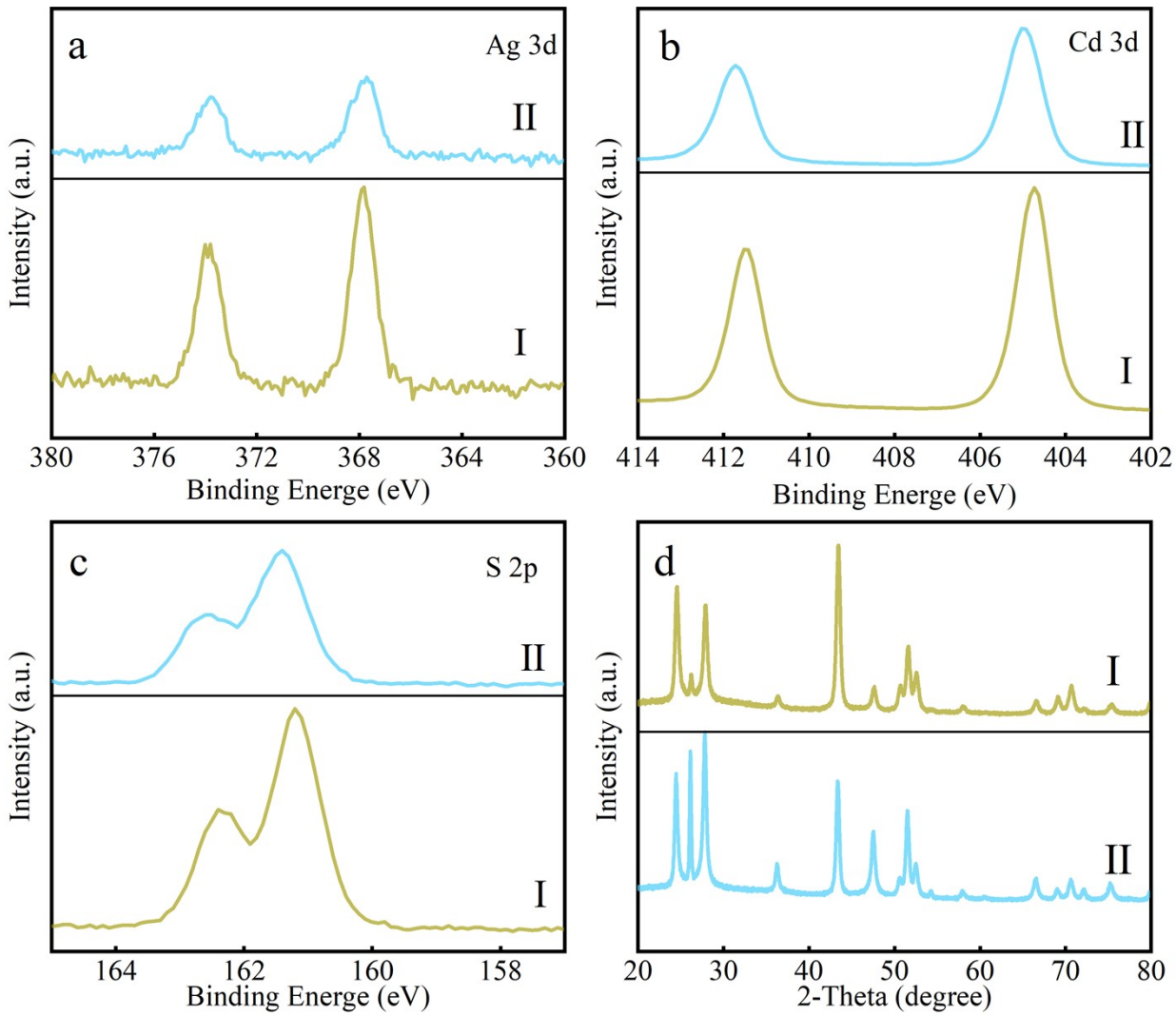

Fig. S10. High-resolution (a) Ag 3d (b)Cd 3d, and (c) S 2p spectra, and (d) XRD patterns spectra of CdS NWs and CdS/$Ag_{25}(SR)_{18}$ heterostructure (I) before and (II) after cyclic 4-NA photoreduction reactions.

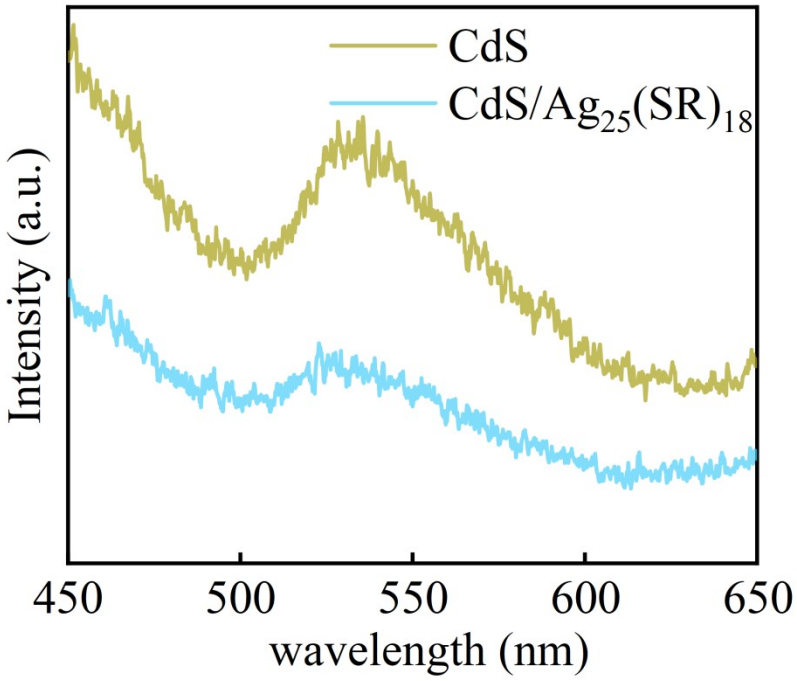

Fig. S11. PL spectra of CdS NWs and CdS/$Ag_{25}(SR)_{18}$ heterostructure with an excitation wavelength of 350 nm

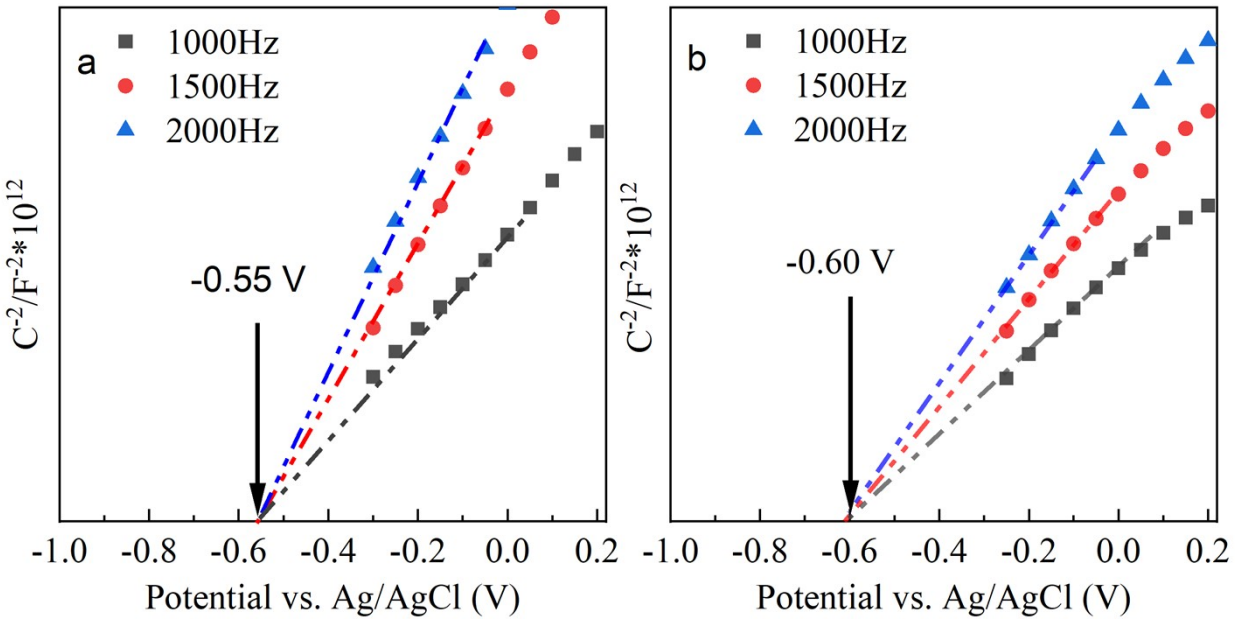

Fig. S12. Mote-Schittky (M-S) plots of (a) CdS NWs and (b) CdS/$Ag_{25}(SR)_{18}$ heterostructure.

Table S1. Peak position of FT-IR with corresponding functional groups.

Peak position (cm^{-1})	*Vibration mode*
3374	$-NH_2$,-OH [2]
2935&2850	$-CH_2$ [2]
1635	$-NH_2$ [2]
1380	$-CH_3$ [2]
1061	-C-N- [2]

Table S2. Chemical bond species for CdS NWs and CdS/$Ag_{25}(SR)_{18}$ heterostructure.

Elements	*CdS*	*CdS/$Ag_{25}(SR)_{18}$*	*Chemical Bond Species*
Cd $3d_{5/2}$	404.82	405.10	Cd^{2+} [3]
Cd $3d_{5/2}$	411.53	411.88	Cd^{2+} [3]
S $2p_{3/2}$	161.28	161.61	S^{2-} [4]
S $2p_{1/2}$	162.46	162.80	S^{2-} [4]
Ag $3d_{5/2}$	N.D.	368.6	Ag^{0} [5; 6]
Ag $3d_{3/2}$	N.D.	374.6	Ag^{0} [5; 6]
Ag $3d_{5/2}$	N.D.	368	Ag^{+} [5; 6]
Ag $3d_{3/2}$	N.D.	374.05	Ag^{+} [5; 6]

N.D.: Not detected

Table S3. Specific surface area, pore volume and pore size of CdS NWs, $CdS/Ag_{25}(SR)_{18}$ heterostructure.

Samples	*SBET (m^2/g)[a]*	*Total pore volume (cm^3/g)[b]*	*Average pore size (nm)*
CdS NWs	30.1736	0.2597	34.4274
$CdS/Ag_{25}(SR)_{18}$	44.6490	0.2783	24.9322

[a] BET surface area is calculated from the linear part of BET plots.
[b] Single point total pore volume of the pores at P/P0=0.99.
[c] Adsorption average pore width (4V/A by BET)

Table S4. Photoactivities of CdS/12%$Ag_{25}(SR)_{18}$ heterostructure toward reduction of nitro compound and Cr^{6+} under visble light irradiation (λ ＞ 420 nm).

Number	*Substrate*	*CdS*	*CdS/$Ag_{25}(SR)_{18}$*
a	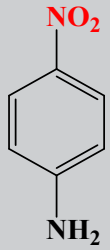	37.59% (5 min)	99.7% (5 min)
b	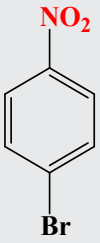	42.09% (1 min)	74.38% (1 min)
c	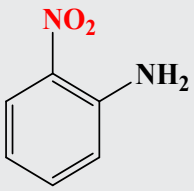	58.17% (5 min)	95.3% (5 min)
d	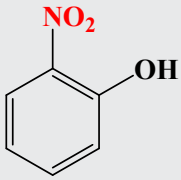	62.48% (5 min)	86.55% (5 min)
e	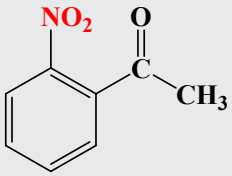	26.03% (2 min)	45.74% (2 min)
f	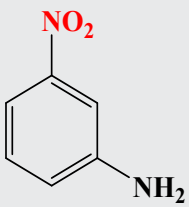	29.11% (2 min)	50.13% (2 min)

g	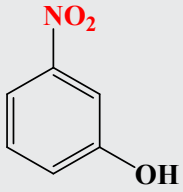	29.1% (5 min)	45.2% (5 min)
h	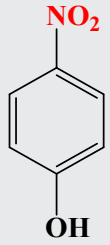	13.53% (5 min)	92.64% (5 min)
i	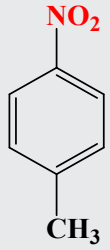	23.65% (3 min)	83.91% (3 min)
j	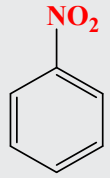	33.94% (2 min)	44.67% (2 min)
k	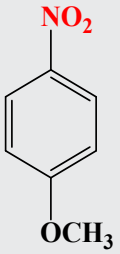	25.09% (3 min)	94.31% (3 min)
l	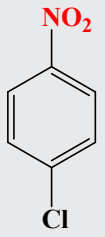	45.81% (2 min)	87.71% (2 min)
m	Cr^{6+}	93.94% (50 min)	99.5% (50 min)

Table S5. Relative element percentage of $CdS/Ag_{25}(SR)_{18}$ heterostructure.

Elements	*Wt (%)*
C	30.13
O	4.8
Cd	50.59
S	12.74
Ag	1.73

References

[1] H. Liang, B. Liu, B. Tang, S. Zhu, S. Li, X. Ge, J. Li, J. Zhu, and F. Xiao, Atomically Precise Metal Nanocluster-Mediated Photocatalysis. ACS Catal. 12 (2022) 4216-4226.

[2] M. Huang, Y. Li, T. Li, X. Dai, S. Hou, Y. He, G. Xiao, and F. Xiao, Self-transformation of Ultra-small Gold Nanoclusters to Gold Nanocrystals toward Boosted Photoreduction Catalysis. Chemical communications (Cambridge, England) 55 (2019) 1591-1594.

[3] R.R. Nasaruddin, M.J. Hülsey, and J. Xie, Enhancing Catalytic Properties of Ligand-protected Gold-based 25-metal Atom Nanoclusters by Silver Doping. Mol. Catal. 518 (2022) 112095.

[4] S. Joardar, M.L. Adams, R. Biswas, G.V. Deodhar, K.E. Metzger, K. Deweese, M. Davidson, R.M. Richards, B.G. Trewyn, and P. Biswas, Direct Synthesis of Silver Nanoparticles Modified Spherical Mesoporous Silica as Efficient Antibacterial Materials. Microporous Mesoporous Mat. 313 (2021) 110824.

[5] W. Liu, X. Wang, H. Yu, and J. Yu, Direct Photoinduced Synthesis of Amorphous CoMoSx Cocatalyst and Its Improved Photocatalytic H_2 -Evolution Activity of CdS. ACS Sustain. Chem. Eng. 6 (2018) 12436-12445.

[6] X. Fu, Y. Li, M. Huang, T. Li, X. Dai, S. Hou, Z. Wei, and F. Xiao, Partially Self-Transformed Transition-Metal Chalcogenide Interim Layer: Motivating Charge Transport Cascade for Solar Hydrogen Evolution. Inorg. Chem. 59 (2020) 2562-2574.